


Cite this: *Mater. Adv.*, 2025,  
6, 2875

# Fluorescent carbon dots with dual emissions and solvent-dependent properties for water detection in organic solvents†

Koki Sekioka,<sup>a</sup> Nazanin Mosleh,<sup>a</sup> Dan Boice,<sup>a</sup> Richard Hailstone<sup>b</sup> and Xiangcheng Sun \*<sup>a</sup>

Detection of water in organic solvents is of importance in both academic and industrial applications. In this work, we developed dual emissive carbon dots (CDs) through a simple solvothermal method using *m*-phenylenediamine and phenolphthalein as precursors. The CDs showed excitation-dependent emission properties with both blue and green emissions. In addition, the CDs' emission peak shifted to longer wavelengths as the polarity of the solvents that dispersed the CDs increased, allowing the CDs to serve as a solvatochromic probe. Besides, the CDs' emissions could be affected by water in different organic solvents, which have been developed as efficient sensors for the detection of trace amounts of water. The limit of detection (LoD) to water detection in ethanol (EtOH), dimethyl sulfoxide (DMSO), and acetonitrile (MeCN) can be as low as 0.12%, 0.01%, and 0.006%, respectively, utilizing the CDs' green emissions. By taking advantage of the dual emissions, the ratiometric detection of water has been achieved. The ratiometric signals could be potentially developed as portable naked-eye based sensors for water detection in organic solvents. The obtained CDs could have promising applications to be used in sensing applications considering their easy synthesis, good optical properties and multi-signals for detection.

Received 9th January 2025,  
Accepted 17th March 2025

DOI: 10.1039/d5ma00021a

rsc.li/materials-advances

## 1. Introduction

All living organisms need water to survive. On the other hand, water is regarded as a common impurity or contaminant in organic solvents.<sup>1</sup> Water is a harmful impurity for many products in the food, medicine, chemical, and energy industries, which may reduce the efficacy and uses of the products.<sup>2,3</sup> In addition, the presence of a trace amount of water in commonly used organic solvents is very frequently encountered, which impedes the reaction process and determines the reaction selectivity and product yield in some organic reactions, leading to detrimental outcomes.<sup>2</sup> Therefore, it is necessary and important to develop a sensor for efficient water detection in organic solvents for industrial applications and synthetic laboratories.<sup>1,2</sup> The traditional method for determining water content is Karl-Fischer titration, achieved by coulometric and volumetric analyses.<sup>4</sup> Several other methods based on chromatography, electrochemistry, and

nuclear magnetic resonance have been developed for water detection as well.<sup>1,5,6</sup> These methods show benefits such as high throughput and great accuracy. However, they are limited by the high cost of specialized equipment, time-consuming assays, and complicated data analysis. Fluorescence-based approaches for water detection have increased extensive attention and have been developed as an alternative due to their operational simplicity, high sensitivity, and low cost.<sup>1,2,4</sup>

Carbon dots (CDs) are a group of carbon-based nanomaterials that were initially discovered in 2004 *via* the purification of arc-discharged synthesized carbon nanotubes.<sup>7,8</sup> CDs typically have a spherical shape with sizes less than 10 nm, and they are primarily comprised of amorphous carbon and/or nanocrystalline regions of sp<sup>2</sup> hybridized graphitic carbon.<sup>8,9</sup> Since the discovery, they have gradually appeared as potential substitutes for other fluorescent materials due to their benefits, such as good fluorescent properties, excellent photostability, low cost, easy synthesis, biocompatibility, and low toxicity.<sup>9–11</sup> These characteristics have enabled them to use in a wide variety of applications for sensing, bio-imaging, optoelectronic devices, and electrocatalysis.<sup>12</sup> Especially, CDs have been developed as efficient chemical sensors, mostly targeting metal ions, anions, small molecules, *etc.*<sup>13</sup>

Recently, fluorescent CDs have been developed as chemical sensors for the efficient detection of trace amounts of water in

<sup>a</sup> Department of Chemical Engineering, Rochester Institute of Technology, Rochester, New York, 14623, USA. E-mail: xgsche@rit.edu

<sup>b</sup> Chester F. Carlson Center for Imaging Science, Rochester Institute of Technology, Rochester, New York, 14623, USA

† Electronic supplementary information (ESI) available. See DOI: <https://doi.org/10.1039/d5ma00021a>



organic solvents. Most previous works utilized single emission fluorescence signals for water detection in organic solvents either through emission intensities<sup>3,5,6,14–18</sup> or emission peak shift.<sup>19–22</sup> However, single emission signals could be affected by the interference of the external environment, resulting in reliability issues.<sup>23</sup> CDs with dual emissions could be developed as chemical sensors with ratiometric signals or multiple functions.<sup>24–27</sup> Until now, there have been only a few studies on dual emissive CDs for water detection in organic solvents with ratiometric or multiple signals.<sup>28</sup> Zheng and the group reported on dual emissive CDs for the detection of water using the changes of two emission peaks. However, only the detection of water in ethanol solvent was investigated.<sup>28</sup> Yan *et al.* proposed dual-emission fluorescent CDs for water detection with water-sensitive red fluorescence signals.<sup>29</sup> The dual-emission carbon dots in this work were obtained by mixing two carbon dots with different emissions. Wu *et al.* prepared carbon dots with dual emissions through a solvothermal synthesis using 2,5-dihydroxyterephthalic acid as a precursor. They achieved ratiometric visual sensing of trace amounts of water in ethanol and some other organic solvents.<sup>1</sup>

In this work, we developed excitation-dependent dual (blue and green) emissive CDs *via* a simple and facile solvothermal method using *m*-phenylenediamine (*m*-PDA) and phenolphthalein as precursors. The synthesized CDs showed solvent-dependent properties, and the emissions shifted to longer wavelengths when the polarity of the solvent that dispersed the CDs increased, which could be used to develop a solvatochromic probe. The green emissions could be more efficiently affected by the presence of water in the organic solvents. The detection of water in various organic solvents was achieved through changes of the green emission as well as ratiometric signals from dual emissions. The sensing mechanisms for water detection were then investigated.

## 2. Experimental section

### 2.1. Reagents and materials

*m*-Phenylenediamine (*m*-PDA), acetonitrile (MeCN), dimethylformamide (DMF), and tetrahydrofuran (THF) were purchased from Sigma-Aldrich. Dimethyl sulfoxide (DMSO), acetone, ethylene glycol (EG), and dichloromethane (DCM) were obtained from VWR. Methanol (MeOH) and phenolphthalein were bought from Fisher Scientific. Ethanol (EtOH) and toluene were purchased from Supelco and Macron, respectively. All reagents were of at least analytical grade and used as received. Ultrapure water (>18.2 MΩ cm) was used to prepare solutions unless mentioned otherwise.

### 2.2. Synthesis of the CDs

CDs were synthesized through a simple solvothermal method. 17 mg of *m*-PDA and 100 mg of phenolphthalein were dissolved in 5 mL of ethanol. The mixture was then transferred into a 50 mL Teflon-lined autoclave reactor and heated at 150 °C for 3 h. After cooling to room temperature, a portion of it was

freeze-dried for characterization, and the rest was stored in the dark and used for other experiments.

### 2.3. Characterization of the CDs

A high-resolution transmission electron microscope (HR-TEM, JEOL JEM-2010) was used to observe the morphology and size of the CDs. X-ray diffraction (XRD) patterns of the CDs were obtained using Bruker D8 XRD instrument operating at 40 kV and 40 mA with a PMMA sample holder. Raman spectra of the CDs were obtained using Bruker-Senterra II under a 633 nm laser. The Fourier transform infrared (FTIR) spectra were collected using an IR Affinity-1 Shimadzu spectrophotometer. The X-ray photoelectron spectroscopy (XPS) spectrum was measured to investigate the elemental composition and surface groups of the CDs. This measurement was carried out using a monochromatic Al K $\alpha$  X-ray source (1486.6 eV). To collect the XPS spectra of the samples, a Thermo Scientific Nexsa XPS Spectrometer was used. A pass energy of 200 eV for survey spectra and 50 eV for high-resolution spectra were used.

The fluorescence spectra were recorded using a Cary Eclipse fluorescence spectrophotometer by Agilent Technologies. The absorption spectra were recorded by a UV-2600 UV-Vis spectrophotometer by Shimadzu. The quantum yield (QY) was calculated utilizing the following equation:<sup>30,31</sup>

$$QY_S = QY_R \frac{I_S OD_R n_S^2}{I_R OD_S n_R^2} \quad (1)$$

The subscripts R and S refer to the reference and the sample, respectively. In this work, the reference fluorophore for green emission was fluorescein dissolved in 0.1 M NaOH, with a known quantum yield of 95%. *I* is the integrated fluorescence intensity of the emission, OD is the optical density of the samples and *n* is the refractive index of the solutions.

### 2.4. Detection of water in organic solvents

Water titration experiments were performed to investigate the change of fluorescence intensities of the CDs in various solvents upon interaction with water. The ethanol of the synthesized CDs solution was removed, and then 2.1 mg of the CDs were dispersed in the cuvette with 3 mL of each organic solvent and mixed homogeneously. Water detection in several solvents, such as EtOH, MeOH, DMSO, and MeCN was investigated. For each water titration, fluorescence spectra at varied water concentrations in organic solvents were collected at their initial optimal excitation wavelength for the green emissions. Depending on the solvent, fluorescence quenching or enhancement of the CD solutions could be observed upon adding water. The quenching efficiency (QE) or enhancement efficiency (EE) was calculated as a function of water concentrations using the following equations:

$$QE = \frac{I_0 - I}{I_0} \quad (2A)$$

$$EE = \frac{I - I_0}{I_0} \quad (2B)$$

where *I*<sub>0</sub> and *I* denote the peak intensities in the absence and



presence of water analytes in various concentrations, respectively. When the addition of water quenches the CDs emissions, QE (quenching efficiency) is used; on the other hand, if the addition of water enhances the CDs emissions, EE (enhancement efficiency) is used. The limit of detection (LoD) to water was calculated for each solvent using the following equation:<sup>3</sup>

$$\text{LoD} = 3 \frac{\text{SD}_{\text{eq}}}{S} \quad (3)$$

where  $\text{SD}_{\text{eq}}$  is the standard deviation of the blank signal and  $S$  is the slope of the linear plot of fluorescence.

For ratiometric detection of water in organic solvents, the CDs were excited at a wavelength of 380 nm to collect fluorescence spectra which include both emission peaks of the CDs solution. Upon addition of water into the CDs solutions, changes in both peaks were observed. The changes in the ratio of two emissions as a function of water concentrations were obtained and utilized as ratiometric sensors for water detection.

### 3. Results and discussion

#### 3.1. Characterization of the CDs

The CDs were synthesized *via* a solvothermal strategy using *m*-phenylenediamine and phenolphthalein as precursors and ethanol as a solvent. The CDs' synthesis conditions (molar ratios and reaction temperature) were optimized considering their quenching efficiency by water, as shown in Table S1 (ESI†). The optimum conditions were determined to be a molar ratio of 1 : 2 for mPDA/phenolphthalein at 150 °C for 3 h. The size and morphology of the prepared CDs were characterized by TEM. Fig. 1A shows a TEM image of the spherical CDs. Lattice

distance of 0.23 nm in the high resolution images was observed, and is shown Fig. 1B. The lattice distance was frequently observed in the CDs and very close to [100] facet of graphene. The particle size distribution shown in Fig. 1C demonstrates that the size of CDs ranges from 2 to 10 nm with two distributions centering at 4.4 nm and 7.3 nm. Fig. 1D shows the XRD pattern of the CDs. A broad peak centered at  $2\theta = 20^\circ$  is consistent with the graphene lattice spacing of 0.43 nm, indicating that the CDs had a lattice structure to some extent, albeit disordered.<sup>5,32</sup> A peak at  $\sim 26^\circ$  is related to the (002) plane of the graphite structure.<sup>33</sup> Besides, many small diffraction peaks are noticeable in the XRD pattern indicating the unsystematic manner of carbon arrangement induced by functional groups on the surface of the CDs.<sup>5,34</sup> The Raman spectrum (Fig. 1E) shows the characteristic D and G bands at  $1370 \text{ cm}^{-1}$  and  $1560 \text{ cm}^{-1}$ . The two bands are related to structural defects and graphitic  $\text{sp}^2$  carbon networks.<sup>32</sup> The measured  $I_{\text{D}}/I_{\text{G}}$  of 0.82 was obtained, indicating an approximately equal amount of defect and graphitized structure. FTIR was used to characterize the composition and functional groups of the CDs. The FTIR spectrum (Fig. 1F) revealed that the CDs have various bonds such as O–H or C–H ( $3100 \text{ cm}^{-1}$ ), C=O ( $1748 \text{ cm}^{-1}$ ), C=C or N–H ( $1614 \text{ cm}^{-1}$ ), C=C ( $1597 \text{ cm}^{-1}$ ), N–O ( $1515 \text{ cm}^{-1}$ ), C–H ( $1465 \text{ cm}^{-1}$  and  $1450 \text{ cm}^{-1}$ ), C–N ( $1279 \text{ cm}^{-1}$ ), C–O or C–N ( $1258 \text{ cm}^{-1}$ ), C–N or C–O ( $1175 \text{ cm}^{-1}$ ), C–O ( $1124 \text{ cm}^{-1}$ ,  $1109 \text{ cm}^{-1}$  and  $1073 \text{ cm}^{-1}$ ), CO–O–CO ( $1037 \text{ cm}^{-1}$ ), C=C ( $925\text{--}960 \text{ cm}^{-1}$ ), C–H or C=C ( $870 \text{ cm}^{-1}$ ), C–H or C=C ( $835 \text{ cm}^{-1}$ ), and C–H ( $758 \text{ cm}^{-1}$  and  $693 \text{ cm}^{-1}$ ).<sup>10,14,35,36</sup>

Furthermore, the elemental composition of the CDs was analyzed by XPS. The survey scan (Fig. 2A) indicated that the CDs consist of C (75.5%), O (15.4%), and N (9.1%). The existence of these three elements (and the absence of others)

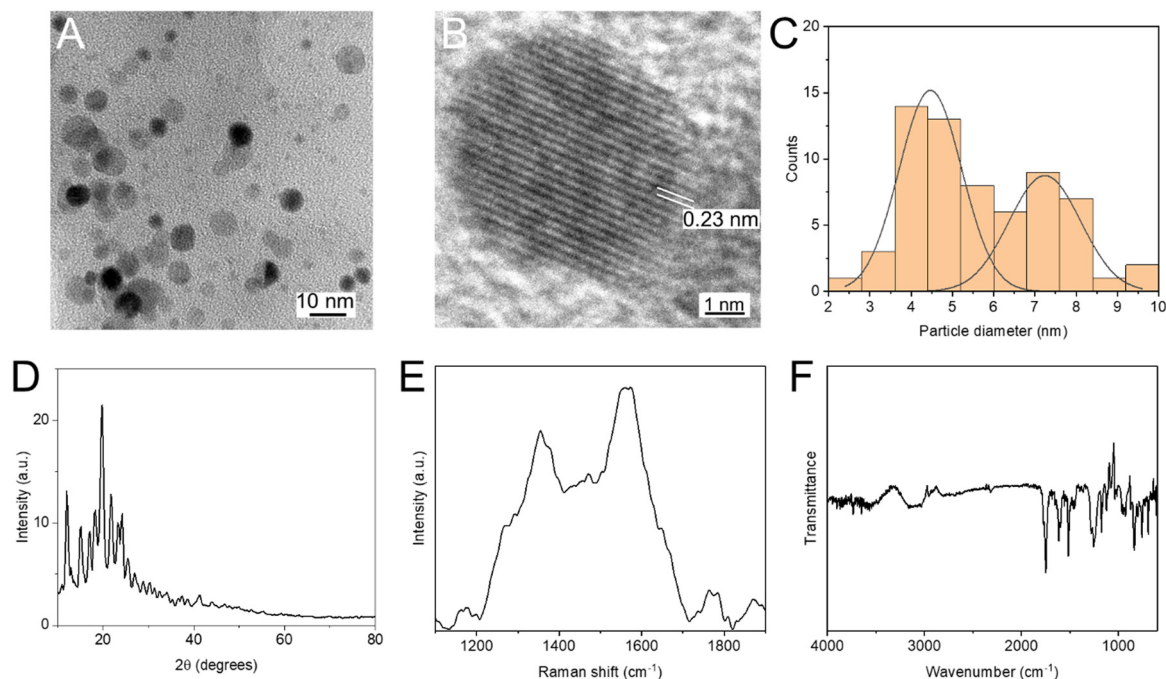


**Fig. 1** Characterization of the synthesized CDs. (A) TEM image of the CDs. (B) HR-TEM images of the CDs with lattice spacings. (C) Size distribution of the CDs. (D) XRD pattern of the CDs. (E) Raman spectrum of the CDs. (F) FTIR spectrum of the CDs dispersed in ethanol.



is consistent with the precursors and synthesis conditions. The high-resolution C 1s spectrum (Fig. 2B) exhibits three peaks with binding energies of 284.6 eV, 285.8 eV, and 287.6 eV, which could be assigned to carbon in the form of C-C/C=C, C-O/C-N, and C=O respectively.<sup>3,17</sup> The high-resolution O 1s spectrum (Fig. 2C) could be de-convoluted into two peaks at 532.4 eV (C=O) and 533.1 eV (C-O). The high-resolution N 1s spectrum (Fig. 2D) shows three peaks with binding energies of 398.8 eV, 399.6 eV, and 400.6 eV, corresponding to N-H, pyridinic/pyrrolic nitrogen, and graphitic nitrogen, respectively.<sup>32</sup>

### 3.2. Optical properties of the CDs

The UV-visible spectrum of the CD solution in ethanol is shown in Fig. 3A. Three peaks were observed, which have been reported by others.<sup>24,37</sup> A strong absorption peak at 278 nm could be attributed to the  $n-\pi$  or  $\pi-\pi^*$  transition of C=C or C=N groups.<sup>24</sup> The other two peaks at  $\sim 353$  and 457 nm with much lower intensities (Inset of Fig. 3A), could be due to the lower energy of extended conjugation structure, which is a helpful indication of long wavelength emission (e.g., the green emission of our CDs).<sup>5,24,38</sup>

The excitation-dependent emission spectra of diluted CDs solution in ethanol were collected and shown in Fig. 3B. When the CDs solution was excited at shorter wavelengths, a blue emission peak at 436 nm was observed, and an excitation of 360 nm resulted in the strongest blue emissions. Increasing the excitation wavelength to 380 nm, two emission peaks at

$\sim 435$  nm and  $\sim 500$  nm were observed. Further extending the excitation wavelength, a major peak at  $\sim 506$  nm was observed, corresponding to the green emission. An excitation of 420 nm leads to the strongest green emission. The results suggest that dual (both blue and green) emissive CDs were obtained, similar to our previous report on the dual emissive carbon dots.<sup>24</sup> The inset shows photographs of the CD solution in ethanol excited with fiber-optics-coupled LEDs of 365 and 455 nm, demonstrating the presence of both blue and green emissions from our developed carbon dots.

The normalized emission spectra excited at 353 nm and 462 nm, and the excitation spectra with emission wavelengths of 506 and 437 nm are shown in Fig. 3C. With an emission wavelength of 506 nm, two major excitation peaks at 460 nm and 365 nm were observed, as well as a minor peak at 315 nm. The emission wavelength of 437 nm leads to an excitation spectrum with a broad peak at  $\sim 360$  nm. The results here suggest at least two major chromophores were present. In addition, the peaks in excitation spectra were consistent with the UV-vis absorption spectra (Fig. 3A) and the peaks that excite the blue and green emissions most efficiently (Fig. 3B).

CDs with dual emissive properties are uncommon. The blue peak can be attributed to the *m*-PDA precursor alone under thermal conditions,<sup>39</sup> while the appearance of green emission in the CDs could be possibly due to the co-precursor phenolphthalein, which leads to varied surface states. In addition, the presence of two size distributions (Fig. 1C) could potentially

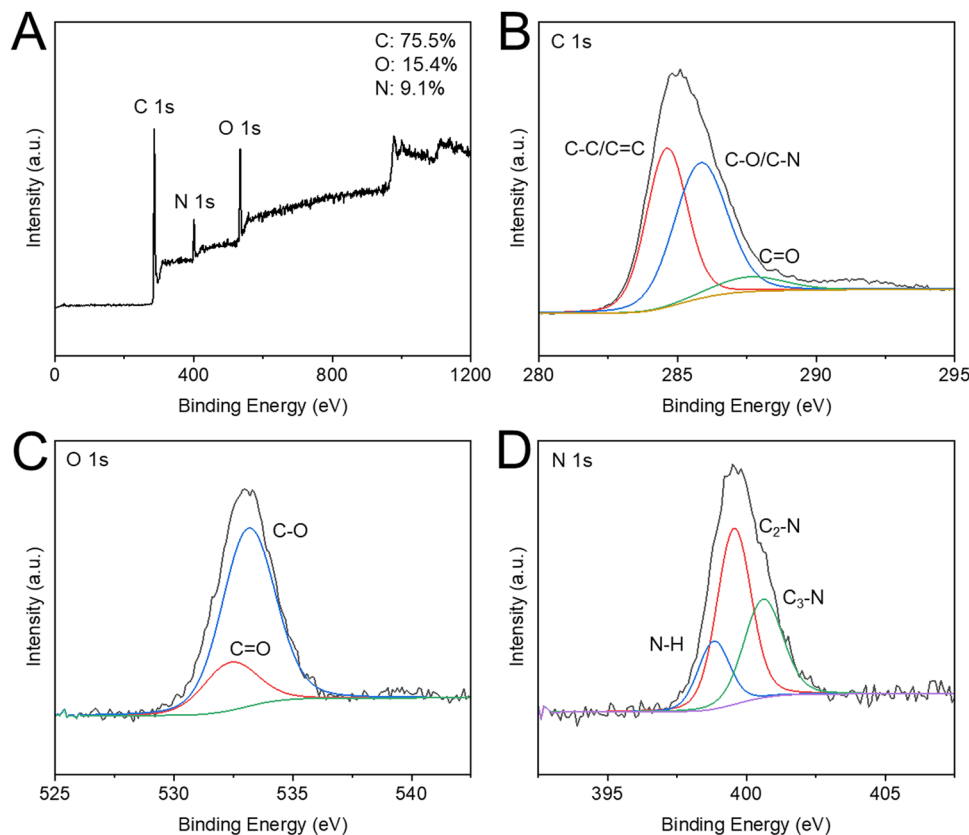
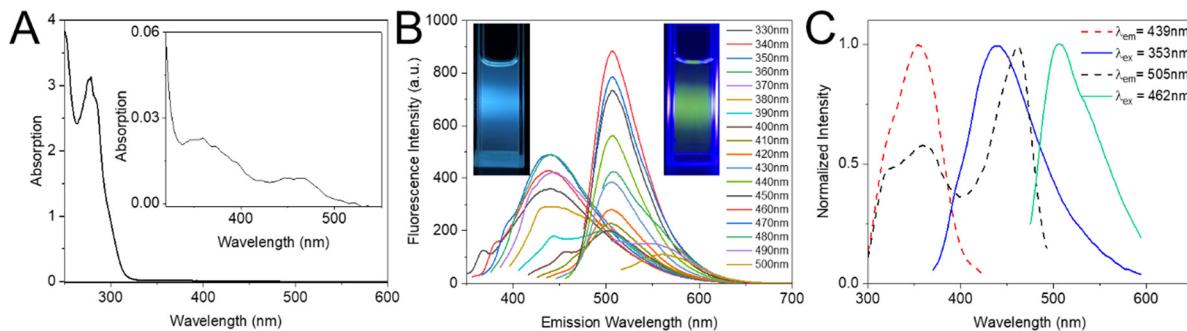


Fig. 2 The XPS spectra of the CDs. (A) Survey scan and high-resolution spectra of (B) C 1s, (C) O 1s, and (D) N 1s peaks.





**Fig. 3** Optical properties of the CDs dispersed in ethanol. (A) Absorption spectra of the CDs in ethanol, inset shows the absorption peaks in the range of 320–550 nm. (B) The fluorescence spectra of the CDs at different excitation wavelengths showing dual emissions. Inset: Photos of CDs showing blue and green emissions under different LED lamps. (C) Normalized emission spectra (solid line) and corresponding excitation spectra (dotted line).

explain the photoluminescence mechanisms for the dual emissions.<sup>9,40</sup> The origin of the dual emissions could be studied through fluorescence at the single-particle level, which is currently considered in our lab. The quantum yield (QY) of the CDs was calculated using eqn (1) with fluorescein as a standard for the green peak. The green peak showed a decent QY of 0.81% in ethanol. QYs in other solvents were also measured and showed similar values around 1–3% (Table S2, ESI<sup>†</sup>).

The CDs showed solvent-dependent properties when we dispersed the CDs in different organic solvents. We found that the blue emissions of the CDs obviously shifted to longer wavelengths when the polarity of solvents increased (Fig. 4A). The green emissions did not show such phenomena obviously (Fig. S1, ESI<sup>†</sup>). Changes in emission wavelengths of the CDs in different solvents are generally attributed to the differences in the relative polarities of the solvents ( $E_T^N$ ).<sup>14</sup> The relationship between the fluorescence emission wavelength and the relative polarities of the solvent is shown in Fig. 4B. The emission peak shifted from 402 nm in Toluene ( $E_T^N$  of 0.1) to 449 nm in methanol ( $E_T^N$  of 0.762). A good linear relation ( $R^2 = 0.892$ ) between peak emission and relative polarity of solvent was obtained.

The phenomenon of solvatochromism is frequently noticed in fluorophore-solvent systems, and the related mechanism was recently studied for CDs in various solvents. According to prior research, the origin of solvatochromism in CDs can be grouped

into two cases:<sup>41</sup> in protic solvents, it is mainly attributed to hydrogen bond interaction between the protic solvent and the CDs;<sup>42,43</sup> on the other hand, in aprotic solvents, it is attributed to a change in the surface electronic state caused by dipole-dipole interactions.<sup>10,44</sup> In aprotic solvents, the dipole moment has more influence on the surface electronic structure with an increase in the solvent polarity, which reduces the energy gap and leads to the emission peak position shifting towards longer wavelengths.<sup>10</sup> Red-shift of fluorescence emission in more polar solvents is consistent with previous reports.<sup>14</sup> The surface has a different energy level structure, and the excited electrons in a highly polar solvent lose more energy than those in the solvents with less polarity, which leads to a red shift of the emission. As the solvent polarity increases, the hydration of carbonyl groups changes the surface states of the CDs. Hydrogen bonds and other specific solvent-fluorophore interactions increase the conjugation degree of the CD system, which results in a decrease in the energy gap for  $\pi$ - $\pi^*$  transitions.<sup>6</sup> Therefore, with the increase of solvent polarity, the CD system shifted its emissions to longer wavelengths.

### 3.3. Detection of water in organic solvents

Water titration experiments were conducted to develop the CDs as a sensor for water detection in organic solvents. When water was gradually added into the CDs solution dispersed in

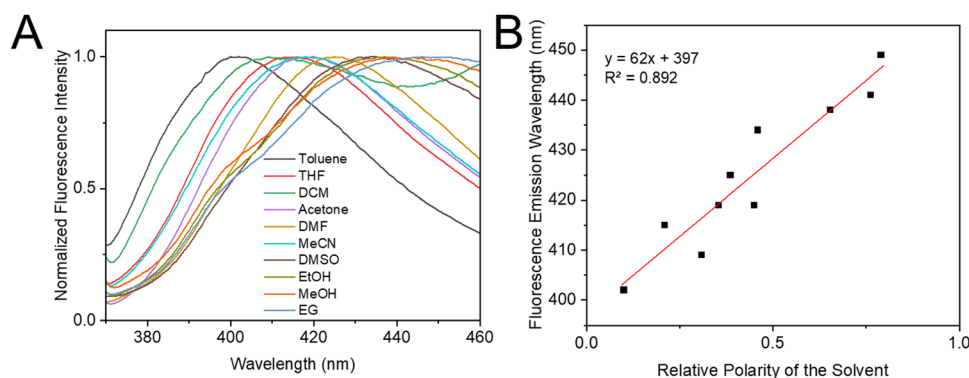


**Fig. 4** Response of the fluorescence emission of the CDs in different organic solvents. (A) Normalized blue emissions of the CDs in the different solvents under excitation of 340 nm. (B) The linear relation between the blue emission peak wavelength and the relative polarity of the solvent.



ethanol, we found that both blue emission and green emissions quenched (under excitation at their corresponding optimum wavelengths), and the green emission peak could be quenched more efficiently by water than that of blue emissions (Fig. 5A and Fig. S2, ESI†). Fig. 5A shows the changes in CDs' fluorescence spectra in ethanol at various concentrations of water. Only 3% of water in the ethanol solvent resulted in about 20% of quenching. And 20% of water in the solvent leads to ~50% quenching efficiency to the CDs. The limit of detection to water detection in ethanol was calculated as low as 0.12%. Water detection in several other organic solvents was realized as well. In DMSO, the CDs demonstrate more efficient fluorescence quenching by water (Fig. 5B). Only 1% water in DMSO resulted in about 80% quenching, and the LoD to water detection in DMSO as low as 0.01% was achieved. Besides, in MeCN, fluorescence enhancement was observed upon interaction with water (Fig. 5C). The normalized fluorescence spectra were also shown in Fig. S3 (ESI†) for direct comparison. Detection of water in other organic solvents such as methanol, DMF, and acetone was achieved as well, and the corresponding quenching or enhancement efficiencies at various concentrations of water are shown in Fig. S4 (ESI†). The developed carbon dots showed good properties (in sensitivity and detection range) to water detection in organic solvents, compared with other recently reported carbon dots for water detection, as summarized in Table S3 (ESI†).

The Stern–Volmer equation (eqn (4A) for quenching and eqn (4B) for enhancement) was used to analyze the quenching (Fig. 5A and B) and enhancement (Fig. 5C) phenomena by water

in EtOH, DMSO, and MeCN, and the results are shown in Fig. 5D–F.

$$\frac{I_0}{I} = 1 + K_{SV}[A] \quad (4A)$$

$$\frac{I}{I_0} = 1 + K_{SV}[A] \quad (4B)$$

where  $K_{SV}$  is the Stern–Volmer constant in  $M^{-1}$ , and  $I_0$  and  $I$  denote the peak intensities in the absence and presence of water analytes at various concentrations  $[A]$ . A linear fitting was observed for the Stern–Volmer plot for fluorescence quenching of the CDs in EtOH by water. Non-linear Stern–Volmer relations were observed for water sensing in DMSO and MeCN. The linear fitting could be attributed to either static or dynamic quenching alone being responsible for the sensing process, whereas the non-linear relationship is generally attributed to the presence of both static and dynamic quenching.<sup>31</sup>

The as-synthesized CDs demonstrated dual emissions, which provide the potential to be developed as ratiometric sensors by taking advantage of changes of the two emissions upon interaction with the analytes. We obtained an emission spectrum with both blue and green emissions by tuning the excitation wavelength (such as 380 nm). The changes of the two emissions of the CDs in ethanol upon interaction with water were investigated. To our surprise, when a 380 nm excitation wavelength was used, the green emissions were enhanced, while the blue emissions were still quenched upon the addition of water (Fig. 6A). A similar phenomenon was observed when

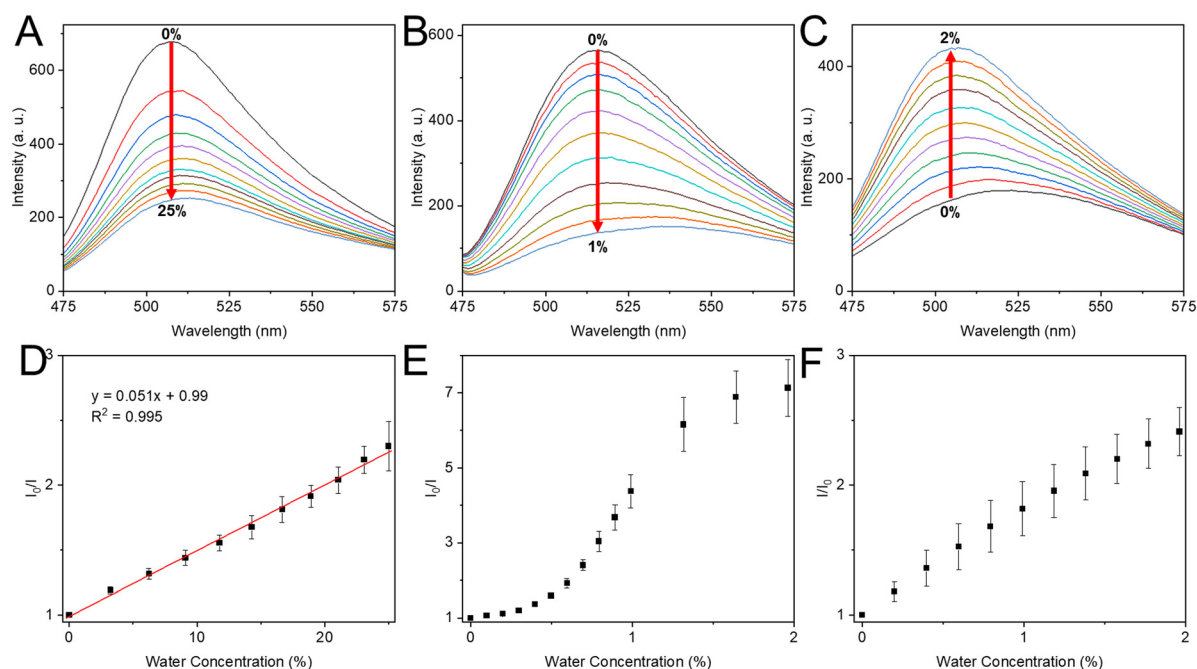


**Fig. 5** Detection of water in different organic solvents with the as-synthesized CDs. Top row: Emission spectra of the green peak under varying water concentrations. Fluorescence spectra of the CDs in different organic solvents ((A) EtOH, (B) DMSO, (C) MeCN) upon addition of water. Bottom row: Stern–Volmer plot for the CDs fluorescence quenching in EtOH (D), DMSO (E), and enhancement in MeCN (F) by water. Optimal excitation wavelengths in each solvent were used: 458 nm for EtOH, 464 nm for DMSO, and 446 nm for MeCN.



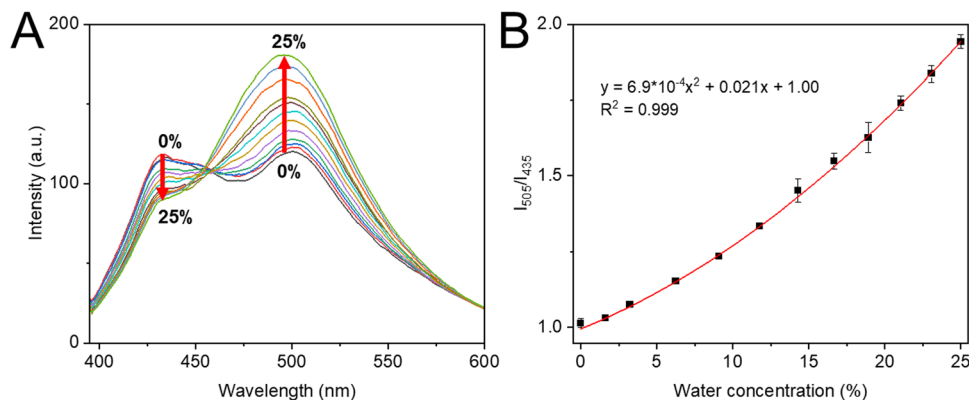


Fig. 6 Ratiometric signals for water detection by the CDs in ethanol with dual emissions. (A) Fluorescence spectra of the CDs in ethanol excited at 380 nm at different concentrations of water. (B) The ratios of two emissions of the CDs in ethanol ( $I_{505}/I_{435}$ ) as a function of water concentrations and the corresponding fitting.

the detection of water was realized using CDs' dual emissions in DMSO (Fig. S5, ESI<sup>†</sup>). The ratiometric signals of  $I_{505}/I_{435}$  as a function of water concentrations were obtained and are shown in Fig. 6B. The intensity ratios increase upon increasing water concentrations, and a second-order polynomial fitting with  $R^2$  as high as 0.999 was realized. The results suggest that the dual emission carbon dots provide ratiometric signals for water detection, which could potentially achieve the detection just through the changes of emission colors and increase the reliability for water detection.<sup>23</sup> And our work present benefits for water detection achievable by changes of single emissions and ratiometric signals from dual emissions, compared with most of the previous reports on carbon dots for water detection *via* changes of single signals (Table S3, ESI<sup>†</sup>). Therefore, our probe presents increased reliabilities for the detection *via* multi-signals.

### 3.4. Sensing mechanism for water detection in organic solvents.

Detections of water in both protic and aprotic solvents were achieved. Addition of water into the CDs/protic solvents such as alcohols, the hydrogen bonding was further enhanced. It is generally believed that hydrogen bond interactions between

protic solvents and CDs are responsible for the CDs' emission properties in the solvents.<sup>43</sup> When water was added, the hydrogen bonding could be changed, thus leading to the changes of CDs' emissions. When water was detected in aprotic solvents *via* the CDs, the electronic states and dipole moments were affected, and CDs' emissions changed.<sup>44</sup>

Changing the surface state of CDs in organic solvents upon the addition of trace amounts of water has been proposed as the sensing mechanism.<sup>6,14</sup> Wu *et al.* reported a sensing mechanism where water molecules reacted with the surfaces of the CDs through the hydration of the carbonyl groups to form a gem-diol species, increasing the density of C-OH groups accordingly.<sup>3</sup> FTIR is one powerful technique to investigate the surface groups of CDs under different conditions.<sup>3,30</sup> In order to understand the sensing mechanism, FTIR spectra of the CDs in ethanol at different concentrations of water were collected and shown in Fig. 7A. We found that FTIR spectra change upon increasing concentrations of water added to the CDs/ethanol solution. For example, the band at  $1037\text{ cm}^{-1}$  gradually decreased and disappeared upon increasing the water concentration, and the peak could correspond to CO-O-CO stretching of anhydride. The observation is consistent with the previous

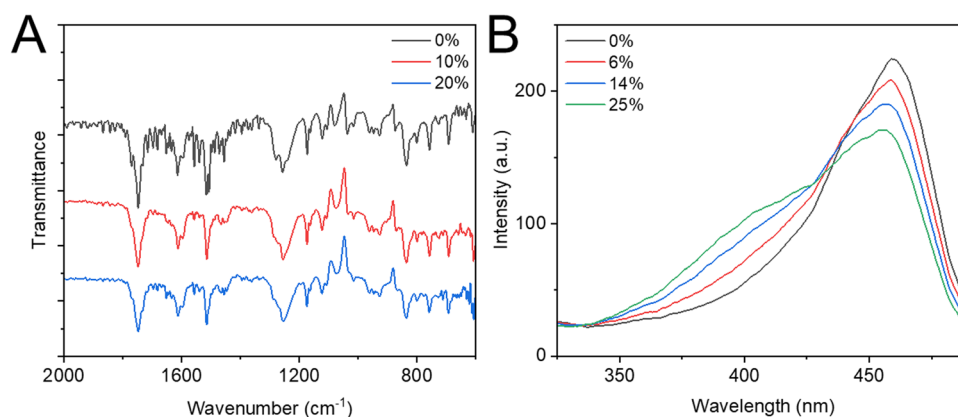


Fig. 7 (A) FTIR spectra of the CDs in ethanol at various concentrations of water. (B) Excitation spectra with emission of 505 nm of the CDs in ethanol at different concentrations of water.



report that the C–O signal is significantly weakened after the addition of water due to the interaction of the CDs with water.<sup>1</sup> The peak at 1279 cm<sup>-1</sup> also gradually decreased upon the addition of water, which could be related to the C–N stretching of aromatic amines. The changes of FTIR spectra for the CDs in DMSO upon the addition of water were also obtained and shown in Fig. S6 (ESI<sup>†</sup>), which could be related to the water detection in another solvent through the CDs.

Furthermore, the reported CDs showed a rare phenomenon where opposite responses (quenching and enhancement) were observed under different excitation wavelengths upon interaction with water. The green emission (at ~505 nm) of the CDs in ethanol was quenched under excitation of 460 nm upon interaction with water, while 380 nm excitation resulted in fluorescence enhancement for the emission. Surface states of the CDs in organic solvents change upon the addition of water and thus affect the excitation spectra, which is directly related to the emission intensities under different irradiations. As such, excitation spectra of the CDs in ethanol with an emission of 505 nm at various concentrations of water were collected (Fig. 7B). We found that as the concentration of water increased, the peak at 380 nm increased, and that at 460 nm decreased, which is consistent with the aforementioned enhancement under excitation at 380 nm (Fig. 6A) and the quenching under 460 nm (Fig. 5A). The origin of the CDs has been related to the surface traps in the radiative transition of carbon dots. Surface groups, such as, C–O, C=O and O=C–OH, can introduce trapping states with different energy levels, making CDs emit light that varies with excitation energy.<sup>45</sup> Recently, Iskandar *et al.* reported on the shift of absorption spectra due to C=O on CDs' surface with DFT simulations.<sup>46</sup> In this work, upon addition of water into the CDs solution in organic solvents, the oxidation states on CDs were modified, which was corroborated by FTIR, resulting in changes of CDs' excitation spectrum. The changes in excitation spectra clearly explain the opposite responses of green emissions under different excitations.

## 4. Conclusions

We have developed dual emissive CDs using *m*-phenylenediamine and phenolphthalein as precursors through a simple solvothermal method. The CDs showed solvent-dependent properties – the emission shifted to longer wavelengths as the polarity of the solvents that dispersed the CDs increased. A linear relation between the emission wavelength and the relative polarity of solvents was observed, and thus the CDs could be developed as solvatochromic probes. In addition, the emission of the CDs in organic solvents could be affected by the addition of trace amounts of water. The presence of trace water resulted in the green emissions' fluorescence quenching for the CDs in EtOH/DMSO and fluorescence enhancement in MeCN. The LODs of water detection could be as low as 0.12% in EtOH, 0.01% in DMSO, and 0.006% in MeCN. In addition, by taking advantage of dual emissions in CDs solutions, the ratiometric sensing of water in organic solvents was achieved. The sensing mechanisms were

proposed, and the surface groups of the CDs as well as the excitation spectra changed upon the addition of water to the CDs organic solutions. The obtained CDs show great potential in chemical sensing applications due to the facile preparation, good optical properties and multiple signals for the detection.

## Data availability

The data supporting this article have been included as part of the ESI.<sup>†</sup>

## Conflicts of interest

There are no conflicts to declare.

## Acknowledgements

The authors would like to thank the Faculty Education and Development (FEAD) Grant and the startup fund from the Rochester Institute of Technology for the financial support.

## Notes and references

- 1 Y. Qin, Y. Bai, P. Huang and F.-Y. Wu, Dual-Emission Carbon Dots for Ratiometric Fluorescent Water Sensing, Relative Humidity Sensing, and Anticounterfeiting Applications, *ACS Appl. Nano Mater.*, 2021, **4**(10), 10674–10681, DOI: [10.1021/acsanm.1c02148](https://doi.org/10.1021/acsanm.1c02148).
- 2 K. Zhang, T.-T. Chen, Y.-J. Shen, L.-F. Zhang, S. Ma and Y. Huang, Luminescent Macrocyclic Sm(III) Complex Probe for Turn-off Fluorescent and Colorimetric Water Detection in Organic Solvents and Liquid Fuels, *Sens. Actuators, B*, 2020, **311**, 127887, DOI: [10.1016/j.snb.2020.127887](https://doi.org/10.1016/j.snb.2020.127887).
- 3 C. Ye, Y. Qin, P. Huang, A. Chen and F.-Y. Wu, Facile Synthesis of Carbon Nanodots with Surface State-Modulated Fluorescence for Highly Sensitive and Real-Time Detection of Water in Organic Solvents, *Anal. Chim. Acta*, 2018, **1034**, 144–152, DOI: [10.1016/j.aca.2018.06.003](https://doi.org/10.1016/j.aca.2018.06.003).
- 4 T.-I. Kim and Y. Kim, A Water Indicator Strip: Instantaneous Fluorogenic Detection of Water in Organic Solvents, Drugs, and Foodstuffs, *Anal. Chem.*, 2017, **89**(6), 3768–3772, DOI: [10.1021/acs.analchem.7b00270](https://doi.org/10.1021/acs.analchem.7b00270).
- 5 Z. Hallaji, Z. Bagheri and B. Ranjbar, One-Step Solvothermal Synthesis of Red Chiral Carbon Dots for Multi-optical Detection of Water in Organic Solvents, *ACS Appl. Nano Mater.*, 2023, **6**(5), 3202–3210, DOI: [10.1021/acsanm.2c04466](https://doi.org/10.1021/acsanm.2c04466).
- 6 Y. Meng, S. Cui, P. Lei, J. Guo, Q. Wang, S. Shuang and C. Dong, Design of Polarity-Dependence Orange Emission Multifunctional Carbon Dots for Water Detection and Anti-Counterfeiting, *Mater. Today Chem.*, 2023, **33**, 101669, DOI: [10.1016/j.mtchem.2023.101669](https://doi.org/10.1016/j.mtchem.2023.101669).
- 7 X. Xu, R. Ray, Y. Gu, H. J. Ploehn, L. Gearheart, K. Raker and W. A. Scrivens, Electrophoretic Analysis and Purification of Fluorescent Single-Walled Carbon Nanotube Fragments,



- J. Am. Chem. Soc.*, 2004, **126**(40), 12736–12737, DOI: [10.1021/ja040082h](https://doi.org/10.1021/ja040082h).
- 8 T. Kuang, M. Jin, X. Lu, T. Liu, H. Vahabi, Z. Gu and X. Gong, Functional Carbon Dots Derived from Biomass and Plastic Wastes, *Green Chem.*, 2023, **25**(17), 6581–6602, DOI: [10.1039/D3GC01763J](https://doi.org/10.1039/D3GC01763J).
  - 9 S. Y. Lim, W. Shen and Z. Gao, Carbon Quantum Dots and Their Applications, *Chem. Soc. Rev.*, 2014, **44**(1), 362–381, DOI: [10.1039/C4CS00269E](https://doi.org/10.1039/C4CS00269E).
  - 10 H. Wang, C. Sun, X. Chen, Y. Zhang, V. L. Colvin, Q. Rice, J. Seo, S. Feng, S. Wang and W. W. Yu, Excitation Wavelength Independent Visible Color Emission of Carbon Dots, *Nanoscale*, 2017, **9**(5), 1909–1915, DOI: [10.1039/C6NR09200D](https://doi.org/10.1039/C6NR09200D).
  - 11 S. Tao, S. Zhu, T. Feng, C. Xia, Y. Song and B. Yang, The Polymeric Characteristics and Photoluminescence Mechanism in Polymer Carbon Dots: A Review, *Mater. Today Chem.*, 2017, **6**, 13–25, DOI: [10.1016/j.mtchem.2017.09.001](https://doi.org/10.1016/j.mtchem.2017.09.001).
  - 12 J. Liu, R. Li and B. Yang, Carbon Dots: A New Type of Carbon-Based Nanomaterial with Wide Applications, *ACS Cent. Sci.*, 2020, **6**(12), 2179–2195, DOI: [10.1021/acscentsci.0c01306](https://doi.org/10.1021/acscentsci.0c01306).
  - 13 X. Sun and Y. Lei, Fluorescent Carbon Dots and Their Sensing Applications, *TrAC, Trends Anal. Chem.*, 2017, **89**, 163–180, DOI: [10.1016/j.trac.2017.02.001](https://doi.org/10.1016/j.trac.2017.02.001).
  - 14 W. Wang, J. Wu, Y. Xing and Z. Wang, Solvent-Dependent Red Emissive Carbon Dots and Their Applications in Sensing and Solid-State Luminescence, *Sens. Actuators, B*, 2022, **360**, 131645, DOI: [10.1016/j.snb.2022.131645](https://doi.org/10.1016/j.snb.2022.131645).
  - 15 J. Wei, H. Li, Y. Yuan, C. Sun, D. Hao, G. Zheng and R. Wang, A Sensitive Fluorescent Sensor for the Detection of Trace Water in Organic Solvents Based on Carbon Quantum Dots with Yellow Fluorescence, *RSC Adv.*, 2018, **8**(65), 37028–37034, DOI: [10.1039/C8RA06732E](https://doi.org/10.1039/C8RA06732E).
  - 16 M. Yang, M. Liu, Z. Wu, Y. He, Y. Ge, G. Song and J. Zhou, Fluorescence Enhanced Detection of Water in Organic Solvents by One-Pot Synthesis of Orange-Red Emissive Polymer Carbon Dots Based on 1,8-Naphthalenediol, *Micro Nano Lett.*, 2020, **15**(7), 469–473, DOI: [10.1049/mnl.2019.0170](https://doi.org/10.1049/mnl.2019.0170).
  - 17 B. Geng, X. Wang, P. Li, W. Shen, H. Qin, F. Fang, L. Yin, L. Shen and D. Pan, Multifunctional Carbon Dots for Trace Water Detection, White LEDs, and Bioimaging, *ChemistrySelect*, 2019, **4**(48), 14162–14168, DOI: [10.1002/slct.201904133](https://doi.org/10.1002/slct.201904133).
  - 18 G. Ma, R. Wang, M. Zhang, Z. Dong, A. Zhang, M. Qu, L. Gao, Y. Wei and J. Wei, Solvothermal Preparation of Nitrogen-Doped Carbon Dots with PET Waste as Precursor and Their Application in LEDs and Water Detection, *Spectrochim. Acta, Part A*, 2023, **289**, 122178, DOI: [10.1016/j.saa.2022.122178](https://doi.org/10.1016/j.saa.2022.122178).
  - 19 A. Senthamizhan, D. Fragouli, B. Balusamy, B. Patil, M. Palei, S. Sabella, T. Uyar and A. Athanassiou, Hydrochromic Carbon Dots as Smart Sensors for Water Sensing in Organic Solvents, *Nanoscale Adv.*, 2019, **1**(11), 4258–4267, DOI: [10.1039/C9NA00493A](https://doi.org/10.1039/C9NA00493A).
  - 20 H. J. Lee, J. Jana, Y.-L. Thi Ngo, L. L. Wang, J. S. Chung and S. H. Hur, The Effect of Solvent Polarity on Emission Properties of Carbon Dots and Their Uses in Colorimetric Sensors for Water and Humidity, *Mater. Res. Bull.*, 2019, **119**, 110564, DOI: [10.1016/j.materresbull.2019.110564](https://doi.org/10.1016/j.materresbull.2019.110564).
  - 21 R. Kumari and S. K. Sahu, Effect of Solvent-Derived Highly Luminescent Multicolor Carbon Dots for White-Light-Emitting Diodes and Water Detection, *Langmuir*, 2020, **36**(19), 5287–5295, DOI: [10.1021/acs.langmuir.0c00631](https://doi.org/10.1021/acs.langmuir.0c00631).
  - 22 Z. Huo, W. Xu, Z. Wang and S. Xu, A Carbonized Polymer Dot (CPD) Nanosensor for Trace Water Detection with a Wide Detection Range, *Dyes Pigm.*, 2021, **196**, 109805, DOI: [10.1016/j.dyepig.2021.109805](https://doi.org/10.1016/j.dyepig.2021.109805).
  - 23 N. Mosleh, L. Hardaker, R. Bartolini and X. Sun, Reaction-Based Multisignal Detection of Palladium with High Sensitivity, Selectivity, and Reliability, *ACS Appl. Opt. Mater.*, 2024, **2**(1), 173–180, DOI: [10.1021/acsaom.3c00391](https://doi.org/10.1021/acsaom.3c00391).
  - 24 X. Sun, C. Brückner and Y. Lei, One-Pot and Ultrafast Synthesis of Nitrogen and Phosphorus Co-Doped Carbon Dots Possessing Bright Dual Wavelength Fluorescence Emission, *Nanoscale*, 2015, **7**(41), 17278–17282, DOI: [10.1039/C5NR05549K](https://doi.org/10.1039/C5NR05549K).
  - 25 Q. Guan, R. Su, M. Zhang, R. Zhang, W. Li, D. Wang, M. Xu, L. Fei and Q. Xu, Highly Fluorescent Dual-Emission Red Carbon Dots and Their Applications in Optoelectronic Devices and Water Detection, *New J. Chem.*, 2019, **43**(7), 3050–3058, DOI: [10.1039/C8NJ06074F](https://doi.org/10.1039/C8NJ06074F).
  - 26 L. Li, L. Shi, J. Jia, O. Eltayeb, W. Lu, Y. Tang, C. Dong and S. Shuang, Dual Photoluminescence Emission Carbon Dots for Ratiometric Fluorescent GSH Sensing and Cancer Cell Recognition, *ACS Appl. Mater. Interfaces*, 2020, **12**(16), 18250–18257, DOI: [10.1021/acsaami.0c00283](https://doi.org/10.1021/acsaami.0c00283).
  - 27 J. Mei, J. Bao, X. Cheng, D. Ren, G. Xu, F. Wei, Y. Sun, Q. Hu and Y. Cen, Novel Dual-Emissive Fluorescent Silicon Nanoparticles for Detection of Enzyme Activity in Supplements Associated with Lactose Intolerance, *Sens. Actuators, B*, 2021, **329**, 129164, DOI: [10.1016/j.snb.2020.129164](https://doi.org/10.1016/j.snb.2020.129164).
  - 28 H. Zou, X. Liao, X. Lu, X. Hu, Y. Xiong, J. Cao, J. Pan, C. Li and Y. Zheng, Fluorescence Studies of Double-Emitting Carbon Dots and Application in Detection of H<sub>2</sub>O in Ethanol and Differentiation of Cancer Cell and Normal Cell, *J. Photochem. Photobiol. Chem.*, 2023, **441**, 114746, DOI: [10.1016/j.jphotochem.2023.114746](https://doi.org/10.1016/j.jphotochem.2023.114746).
  - 29 X. Liu, Z. Zhou, T. Wang, P. Deng and Y. Yan, Visual Monitoring of Trace Water in Organic Solvents Based on Ecofriendly b/r-CDs Ratiometric Fluorescence Test Paper, *Talanta*, 2020, **216**, 120958, DOI: [10.1016/j.talanta.2020.120958](https://doi.org/10.1016/j.talanta.2020.120958).
  - 30 X. Sun, J. He, Y. Meng, L. Zhang, S. Zhang, X. Ma, S. Dey, J. Zhao and Y. Lei, Microwave-Assisted Ultrafast and Facile Synthesis of Fluorescent Carbon Nanoparticles from a Single Precursor: Preparation, Characterization and Their Application for the Highly Selective Detection of Explosive Picric Acid, *J. Mater. Chem. A*, 2016, **4**(11), 4161–4171, DOI: [10.1039/C5TA10027E](https://doi.org/10.1039/C5TA10027E).
  - 31 *Principles of Fluorescence Spectroscopy*, ed., Lakowicz, J. R., Springer US, Boston, MA, 2006, DOI: [10.1007/978-0-387-46312-4](https://doi.org/10.1007/978-0-387-46312-4).
  - 32 A. McEnroe, E. Brunt, N. Mosleh, J. Yu, R. Hailstone and X. Sun, Bright, Green Fluorescent Carbon Dots for Sensitive and Selective Detection of Ferrous Ions, *Talanta Open*, 2023, **7**, 100236, DOI: [10.1016/j.talo.2023.100236](https://doi.org/10.1016/j.talo.2023.100236).
  - 33 S. Wei, L. Tan, X. Yin, R. Wang, X. Shan, Q. Chen, T. Li, X. Zhang, C. Jiang and G. Sun, A Sensitive “ON–OFF”



- Fluorescent Probe Based on Carbon Dots for Fe<sup>2+</sup> Detection and Cell Imaging, *Analyst*, 2020, **145**(6), 2357–2366, DOI: [10.1039/C9AN02309G](https://doi.org/10.1039/C9AN02309G).
- 34 S. Thulasi, A. Kathiravan and M. Asha Jhonsi, Fluorescent Carbon Dots Derived from Vehicle Exhaust Soot and Sensing of Tartrazine in Soft Drinks, *ACS Omega*, 2020, **5**(12), 7025–7031, DOI: [10.1021/acsomega.0c00707](https://doi.org/10.1021/acsomega.0c00707).
- 35 Infrared Spectroscopy Absorption Table. Chemistry LibreTexts. [https://chem.libretexts.org/Ancillary\\_Materials/Reference/Reference\\_Tables/Spectroscopic\\_Reference\\_Tables/Infrared\\_Spectroscopy\\_Absorption\\_Table](https://chem.libretexts.org/Ancillary_Materials/Reference/Reference_Tables/Spectroscopic_Reference_Tables/Infrared_Spectroscopy_Absorption_Table) (accessed 2024-11-06).
- 36 Y. Nie, W. Lai, N. Zheng and W. Weng, Multifunctional Room-Temperature Phosphorescent Carbon Dots for Relative Humidity Determination and Information Encryption, *Talanta*, 2021, **233**, 122541, DOI: [10.1016/j.talanta.2021.122541](https://doi.org/10.1016/j.talanta.2021.122541).
- 37 H. Nie, M. Li, Q. Li, S. Liang, Y. Tan, L. Sheng, W. Shi and S. X.-A. Zhang, Carbon Dots with Continuously Tunable Full-Color Emission and Their Application in Ratiometric pH Sensing, *Chem. Mater.*, 2014, **26**(10), 3104–3112, DOI: [10.1021/cm5003669](https://doi.org/10.1021/cm5003669).
- 38 Y. Liu, H. Yang, C. Ma, S. Luo, M. Xu, Z. Wu, W. Li and S. Liu, Luminescent Transparent Wood Based on Lignin-Derived Carbon Dots as a Building Material for Dual-Channel, Real-Time, and Visual Detection of Formaldehyde Gas, *ACS Appl. Mater. Interfaces*, 2020, **12**(32), 36628–36638, DOI: [10.1021/acsaami.0c10240](https://doi.org/10.1021/acsaami.0c10240).
- 39 K. Jiang, S. Sun, L. Zhang, Y. Lu, A. Wu, C. Cai and H. Lin, Red, Green, and Blue Luminescence by Carbon Dots: Full-Color Emission Tuning and Multicolor Cellular Imaging, *Angew. Chem., Int. Ed.*, 2015, **54**(18), 5360–5363, DOI: [10.1002/anie.201501193](https://doi.org/10.1002/anie.201501193).
- 40 D. Ozyurt, M. A. Kobaisi, R. K. Hocking and B. Fox, Properties, Synthesis, and Applications of Carbon Dots: A Review, *Carbon Trends*, 2023, **12**, 100276, DOI: [10.1016/j.cartre.2023.100276](https://doi.org/10.1016/j.cartre.2023.100276).
- 41 S. Mei, X. Wei, Z. Hu, C. Wei, D. Su, D. Yang, G. Zhang, W. Zhang and R. Guo, Amphiphilic Carbon Dots with Solvent-Dependent Optical Properties and Sensing Application, *Opt. Mater.*, 2019, **89**, 224–230, DOI: [10.1016/j.optmat.2019.01.021](https://doi.org/10.1016/j.optmat.2019.01.021).
- 42 S. Mukherjee, E. Prasad and A. Chadha, H-Bonding Controls the Emission Properties of Functionalized Carbon Nanodots, *Phys. Chem. Chem. Phys.*, 2017, **19**(10), 7288–7296, DOI: [10.1039/C6CP08889A](https://doi.org/10.1039/C6CP08889A).
- 43 T. Zhang, J. Zhu, Y. Zhai, H. Wang, X. Bai, B. Dong, H. Wang and H. Song, A Novel Mechanism for Red Emission Carbon Dots: Hydrogen Bond Dominated Molecular States Emission, *Nanoscale*, 2017, **9**(35), 13042–13051, DOI: [10.1039/C7NR03570E](https://doi.org/10.1039/C7NR03570E).
- 44 A. Pramanik, S. Biswas and P. Kumbhakar, Solvatochromism in Highly Luminescent Environmental Friendly Carbon Quantum Dots for Sensing Applications: Conversion of Bio-Waste into Bio-Asset, *Spectrochim. Acta, Part A*, 2018, **191**, 498–512, DOI: [10.1016/j.saa.2017.10.054](https://doi.org/10.1016/j.saa.2017.10.054).
- 45 X. Li, S. Zhang, S. A. Kulinich, Y. Liu and H. Zeng, Engineering Surface States of Carbon Dots to Achieve Controllable Luminescence for Solid-Luminescent Composites and Sensitive Be<sup>2+</sup> Detection, *Sci. Rep.*, 2014, **4**(1), 4976, DOI: [10.1038/srep04976](https://doi.org/10.1038/srep04976).
- 46 R. Umami, F. A. Permatasari, C. D. D. Sundari, F. Muttaqien and F. Iskandar, Surface Functional Groups Effect on the Absorption Spectrum of Carbon Dots: Initial TD-DFT Study, *J. Phys. Conf. Ser.*, 2022, **2243**(1), 012043, DOI: [10.1088/1742-6596/2243/1/012043](https://doi.org/10.1088/1742-6596/2243/1/012043).

